# A New Family of Quaternary, Early Rare-Earth Chalcogenides: $Ca_4(RE)_2In_4Q_{13}$ (RE = La, Nd, Sm, Gd; Q = S, Se)

**James D. Carpenter and Shiou-Jyh Hwu*,†**

Department of Chemistry, Rice University, P.O. Box 1892, Houston, Texas 77251

*Received March 8, 1995*[⊗]

A new family of mixed-metal chalcogenides containing early rare-earth (RE) elements has been synthesized, *e.g.*, $Ca_4(RE)_2In_4Q_{13}$ (RE = La, Nd, Sm, Gd; Q = S, Se). X-ray analysis showed that these compounds crystallize in an orthorhombic crystal system with the space group *Pbam* (No. 55); $Z = 4$. Four of the title compounds, being synthesized in single-crystal form via an eutectic halide flux method, were examined by X-ray single crystal diffraction methods. The indexed cell dimensions are $a = 20.420$ (3) Å, $b = 25.447$ (6) Å, and $c = 3.934$ (2) Å for $Ca_4Nd_2In_4S_{13}$ (**1**), $a = 21.348$ (4) Å, $b = 26.562$ (6) Å, and $c = 4.096$ (3) Å for $Ca_4Nd_2In_4Se_{13}$ (**2**) $a = 21.348$ (3) Å, $b = 26.483$ (6) Å, and $c = 4.077$ (2) Å for $Ca_4Sm_2In_4Se_{13}$ (**3**), and $a = 21.249$ (3) Å, $b = 26.353$ (5) Å, $c = 4.057$ (3) Å for $Ca_4Gd_2In_4Se_{13}$ (**4**). The structural and thermal parameters were refined by full-matrix least-squares methods to $R/R_w$/GOF (based on $F$ with 142 variables) = 0.040/0.047/1.39 (**1**), 0.040/0.043/1.27 (**2**), 0.036/0.041/1.31 (**3**), and 0.051/0.056/1.44 (**4**). The structure consists of cation-centered Ca–Q octahedra, (RE/Ca)–Q bicapped trigonal prisms, and In–Q tetrahedra and octahedra. Detailed studies reveal that these new phases are nonstoichiometric with respect to cation mixing, giving rise to a general formula of $Ca_{2+x}(RE)_{4-x}In_4Q_{13}$ ($x \sim 2.0$). The title compounds are isostructural with the $Pb_4In_2Bi_4S_{13}$ phase in the sense that the corresponding chemical formula can be written as $(Bi_2Pb_x)Pb_{4-x}(In_2Bi_2)S_{13}$ ($x = 2$). The results of differential thermal analysis suggest that these new chalcogenides melt congruently under vacuum. The anomalous lower thermal stability for sulfides compared to selenides observed in thermogravimetric analyses is attributed to an oxidative decomposition to complex sulfates at elevated temperatures. Preliminary optical bandgap measurements of selected phases show medium-gapped semiconductors with $E_g$ of ~2.0 eV for sulfides and ~1.2 eV for selenides. Structure and property comparisons between the $CaYbInQ_4$ and $Ca_4(RE)_2In_4Q_{13}$ families are briefly discussed.

## Introduction

Through synthesis employing molten halide fluxes, several novel mixed-metal chalcogenides have been isolated in single-crystal form for structure and property examinations.[1-4] In systems containing rare-earth (RE) elements, an abundant structural chemistry has been revealed due to the adaptive nature of $(RE)Q_n$ polyhedra. In the ternary $A(RE)_2Q_4$ chalcogenide series,[5] early studies via powder X-ray diffraction methods showed that four structural types were adopted. Chalcogenides ($Q^{2-} = S^{2-}$, $Se^{2-}$) with A = Sr and Ba were discovered in the $Th_3P_4$[6] and $CaFe_2O_4$[7] types for early vs late $RE^{3+}$ cations, respectively. As to compounds based on the A = Ca, three structural types were adopted, $Yb_3S_4$ (low temperature),[8] $MnYb_2S_4$ (high temperature),[9] and $Th_3P_4$, depending upon both the size of the RE cations and reaction conditions. Recent successes in using molten-salt methods have allowed the $A(RE)_2Q_4$ structures to be reexamined. Except for the $MnYb_2S_4$ type, all others have been confirmed by X-ray single-crystal methods.[2a,b,d] New phenomena concerning nonstoichiometry with respect to either cation mixing, $Ca_{1-x}Yb_{2+x}S_4$, or cation/anion deficiency, $Ba_{1-x}Sm_2S_{4-x}$, have been addressed.

The current study stemmed from our continued interest in exploring quaternary chalcogenides to seek better ceramics with enhanced properties which are important to device applications. Some members of the $A(RE)_2Q_4$ family have been investigated for potential applications as optical window materials.[10] Our recent studies have shown that incorporation of RE cations may be beneficial[2c,d] with respect to acquiring extended thermal stability against decomposition in an oxygen-containing atmosphere. This has motivated us to further study the role of RE cations in the phase formation of quaternary chalcogenide systems. In an attempt to synthesize analogs of the $CaYbInQ_4$ series,[2c] a new family of mixed-metal chalcogenides containing

† Permanent address: Department of Chemistry, Clemson University, Clemson, SC 29634.

⊗ Abstract published in *Advance ACS Abstracts*, August 1, 1995.

(1) (a) Kipp, D. O.; Lowe-Ma, C. K.; Vanderah, T. A. *Chem. Mater.* **1990**, *2*, 506. (b) Lowe-Ma, C. K.; Kipp, D. O.; Vanderah, T. A. *J. Solid State Chem.* **1991**, *92*, 520.

(2) (a) Carpenter, J. D.; Hwu, S.-J. *J. Solid State Chem.* **1992**, *97*, 332. (b) Carpenter, J. D.; Hwu, S.-J. *Acta Crystallogr.* **1992**, *C48*, 1164. (c) Carpenter, J. D.; Hwu, S.-J. *Chem. Mater.* **1992**, *4*, 1368. (d) Carpenter, J. D. Ph.D. Dissertation, Rice University, 1993.

(3) (a) Bucher, C. K.; Hwu, S.-J. *Inorg. Chem.* **1994**, *33*, 5831. (b) Hwu, S.-J.; Bucher, C. K.; Carpenter, J. D.; Taylor, S. P. *Inorg. Chem.* **1995**, *34*, 1979.

(4) (a) Hung, Y.-C.; Hwu, S.-J. *Acta Crystallogr.* **1993**, *C49*, 1588. (b) Hung, Y.-C.; Hwu, S.-J. *Inorg. Chem.* **1993**, *32*, 5427. (c) Hung, Y.-C. Ph.D. Dissertation, Rice University, 1994.

(5) (a) Patrie,.M.; Golabi, S. M.; Flahaut, J.; Domange, L. *C. R. Acad. Sci. Paris* **1964**, *259*, 4039. (b) Patrie, M.; Flahaut, J.; Chaudron, G. *C. R. Acad. Sci. Paris* **1967**, *264*, 395.

(6) Meisel, K. *Z. Anorg. Allg. Chem.* **1939**, *240*, 300.

(7) Decker, B. F.; Kasper, J. S. *Acta Crystallogr.* **1957**, *10*, 332.

(8) Chevalier, R.; Laruelle, P.; Flahaut, J. *Bull. Soc. Fr. Minéral. Crystallogr.* **1967**, *90*, 564.

(9) Heikens, H. H.; Kuindersma, R. S.; van Bruggen, C. F.; Haas, C. *Phys. Status Solidi A* **1978**, *46*, 687.

(10) (a) White, W. B.; Chess, C. A.; Chess, D. L.; Biggers, J. V. *Proc. SPIE-Int. Soc. Opt. Eng.* **1981**, *297*, 38. (b) Chess, D. L.; Chess, C. A.; Biggers, J. V.; White, W. B. *J. Am. Ceram. Soc.* **1983**, *66*, 18. (c) Chess, D. L.; Chess, C. A.; White, W. B. *Mater. Res. Bull.* **1984**, *19*, 1551. (d) Saunders, K. J.; Wong, T. Y.; Hartnett, T. M.; Tustison, R. W.; Gentilmen, R. L. *Proc. SPIE-Int. Soc. Opt. Eng.* **1986**, *683*, 72. (e) Savage, J. A.; Lewis, K. L.; Kinsman, B. E.; Wilson, A. R.; Riddle, R. *Proc. SPIE-Int. Soc. Opt. Eng.* **1986**, *683*, 79. (f) Harris, D. C.; Hills, M. E.; Gentilmen, R. L.; Saunders, K. J.; Wong, T. Y. *Adv. Ceram. Mater.* **1987**, *2*, 74. (g) Provenzano, P. L.; White, W. B. *J. Am. Ceram. Soc.* **1990**, *73*, 1766.

0020-1669/95/1334-4647$09.00/0 

**Table 1.** Crystallographic Data for $Ca_4Nd_2In_4S_{13}$ and $Ca_4(RE)_2In_4Se_{13}$ (RE =Nd, Sm, Gd)

| chemical formula | $Ca_{3.7}Nd_{2.3}In_4S_{13}$ | $Ca_{3.7}Nd_{2.3}In_4Se_{13}$ | $Ca_{4.1}Sm_{1.9}In_4Se_{13}$ | $Ca_{3.6}Gd_{2.4}In_4Se_{13}$ |
|---|---|---|---|---|
| fw[a] | 1357.16 | 1965.81 | 1935.75 | 2007.45 |
| space group | *Pbam* (No. 55) | *Pbam* (No. 55) | *Pbam* (No. 55) | *Pbam* (No. 55) |
| *a*, Å | 20.420(3) | 21.348(4) | 21.348(3) | 21.249(4) |
| *b*, Å | 25.447(6) | 26.562(6) | 26.483(6) | 26.353(5) |
| *c*, Å | 3.934(2) | 4.096(3) | 4.077(2) | 4.057(3) |
| *V*, Å$^3$ | 2044(1) | 2322(2) | 2305(1) | 2272(2) |
| *Z* | 4 | 4 | 4 | 4 |
| *T*, °C | 23 | 23 | 23 | 23 |
| $\varrho_{calc}$,[a] g cm$^{-3}$ | 4.41 | 5.63 | 5.58 | 5.87 |
| $\lambda$, Å | 0.710 69 | 0.710 69 | 0.710 69 | 0.710 69 |
| linear abs coeff, cm$^{-1}$ | 249.85 | 307.72 | 405.04 | 327.39 |
| $R$[b] | 0.040 | 0.040 | 0.036 | 0.051 |
| $R_w$[c] | 0.047 | 0.043 | 0.041 | 0.056 |

[a] Calculated based upon the refined structural formula (see text). [b] $R = \Sigma[|F_o| - |F_c|]/\Sigma|F_o|$. [c] $R_w = [\Sigma w[|F_o| - |F_c|]^2/\Sigma w|F_o|^2]^{1/2}$.

early lanthanides has been discovered, *i.e.*, $Ca_4(RE)_2In_4Q_{13}$ (RE = La, Nd, Sm, Gd; Q = S, Se). Synthesis, structure, thermal properties, and preliminary results of optical spectroscopy of these newly discovered chalcogenides are presented.

## Experimental Section

**Synthesis.** Dark-red sulfide and black selenide single crystals were grown using the two-step flux method previously described.[2c] The starting materials, by weight of ca. 0.5 g total, were CaQ (Q = S, 99.99%, and Se, 99.5%; Aesar), rare-earth metals (RE = La, Nd, Sm, and Gd; Aesar and Aldrich 99.9%), In (Aldrich, 99.999%), and Q (Q = S, Se; Aldrich and Strem 99.99%), in molar ratios of 1:1:1:3. In the first step, reaction mixtures were heated at a rate of ca. 10 °C per hour to 950 °C, followed by annealing for 6 days, and then furnace cooled to room temperature. The intimately mixed polycrystalline materials, showing an unidentifiable X-ray powder diffraction pattern, were used as precursors for the single-crystal growth in the following step. The eutectic halide flux of 74/26 mol % of $CaCl_2$/KCl (mp 640 °C) was employed. The precursor/flux mixture (in a mass ratio of 1:4) was heated to 1000 °C at a rate of ca. 60 °C per hour, held at this temperature for 6 days, cooled at a rate of 1.5 °C per hour to 600 °C, and then cooled to room temperature over a 24 h period. Needle crystals were isolated from the flux by washing the reaction products with deionized water. Qualitative elemental analysis of single crystals was performed via energy dispersive spectroscopy (EDS) and showed no extraneous elements.

Polycrystalline materials of the $Ca_4(RE)_2In_4Q_{13}$ family were prepared using procedures described in step one above. Stoichiometric reactants were first ground in a $N_2$-purged drybox and then sealed in a fused silica ampule under vacuum. This was heated at 950 °C for a period of 10−14 days, and regrind/reseal/reheat procedures were followed until completion.

**X-ray Single-Crystal Structure Determination.** Four phases were examined by a Rigaku AFC5S four circle X-ray diffractometer. The summary of crystallographic data is listed in Table 1, and a detailed table is given in the supplementary material. The data collection procedures were the same as previously reported.[2c] On the basis of the intensity statistics, as well as the successful solution and structure refinements, the space group was determined to be *Pbam*. Lorentz−polarization and empirical absorption corrections were applied to the intensity data. The atomic coordinates were found by the PATTERSON method using the program SHELXS-86.[11] The structural and anisotropic thermal parameters were refined by full-matrix least-squares methods, using the TEXSAN software package.[12] Initially the refined structural formula was "$Ca_2(RE)_4In_4Se_{13}$" based on the relative intensities of the Fourier map. The multiplicities for all the atoms were refined but the resultant values indicated nonstoichiometry only on the RE sites. Subsequent refinements, including the secondary extinction,[13] resulted in a much improved structure solution. The refinements (based on *F*) for the neodymium-containing selenide structure, for example, gave $R = 0.083$, $R_w = 0.127$, and GOF = 3.69 for $Ca_2Nd_4In_4Se_{13}$, and $R = 0.040$, $R_w = 0.043$, GOF = 1.27 for $Ca_{2-x}Nd_{4-x}In_4Se_{13}$, $x = 1.7$. The nonstoichiometric Ca ($x$) in the formula is derived on the basis of mixed (Ca, Nd) sites from the refined multiplicities of the four Nd atoms. According to charge neutrality and the below powder X-ray analysis, the empirical formula is rounded off as $Ca_4Nd_2In_4Se_{13}$. Since the title compounds are isostructural, the final positional and thermal parameters for the $Ca_4Nd_2In_4Se_{13}$ phase only are listed in Table 2. For simplicity, in later discussions the mixed (Ca, Nd) site is represented by Nd.

**Table 2.** Positional and Isotropic Thermal Parameters for $Ca_4Nd_2In_4Se_{13}$

| atom | *x* | *y* | *z* | $B_{eq}$,[a] Å$^2$ |
|---|---|---|---|---|
| Ca(1) | 0.1124(2) | 0.0877(1) | 1/2 | 1.2(2) |
| Ca(2) | 0.3437(2) | 0.0199(1) | 1/2 | 1.3(2) |
| Nd(1)[b] | 0.32701(6) | 0.27459(5) | 1/2 | 0.90(5) |
| Nd(2)[b] | 0.12036(7) | 0.24939(6) | 1/2 | 0.87(5) |
| Nd(3)[b] | 0.32649(7) | 0.43398(5) | 1/2 | 0.98(6) |
| Nd(4)[b] | 0.46833(7) | 0.14959(6) | 1/2 | 1.01(6) |
| In(1) | 0.47885(6) | 0.33812(6) | 0 | 1.78(6) |
| In(2) | 0 | 0 | 0 | 2.6(1) |
| In(3) | 0.15302(7) | 0.38934(5) | 0 | 1.66(6) |
| In(4) | 0.27287(6) | 0.15308(5) | 0 | 1.21(5) |
| In(5) | 0 | 1/2 | 0 | 3.6(1) |
| Se(1) | 0.35659(8) | 0.35419(7) | 0 | 0.95(7) |
| Se(2) | 0.47752(9) | 0.42328(7) | 1/2 | 1.42(8) |
| Se(3) | 0.10192(8) | 0.16487(7) | 0 | 0.93(7) |
| Se(4) | 0.47355(9) | 0.27283(7) | 1/2 | 1.25(8) |
| Se(5) | 0.12149(9) | 0.00955(7) | 0 | 1.09(7) |
| Se(6) | 0.06362(8) | 0.31913(7) | 0 | 0.92(7) |
| Se(7) | 0.0660(1) | 0.43936(8) | 1/2 | 1.59(8) |
| Se(8) | 0.2132(1) | 0.34754(8) | 1/2 | 1.56(8) |
| Se(9) | 0.22884(9) | 0.46842(7) | 0 | 0.98(7) |
| Se(10) | 0.38006(8) | 0.19753(7) | 0 | 0.97(7) |
| Se(11) | 0.22734(9) | 0.24300(7) | 0 | 0.99(7) |
| Se(12) | 0.2483(1) | 0.09762(7) | 1/2 | 1.15(7) |
| Se(13) | 0.41889(9) | 0.07201(7) | 0 | 1.11(7) |

[a] Anisotropically refined atoms are given in the form of the isotropic equivalent displacement parameters defined as $B_{eq} = (8\pi^2/3)$ trace *U*. [b] The occupancy factors were first refined with fixed thermal parameters. The multiplicities of Ca/Nd on the Nd sites were fixed for the final refinements, *i.e.*, 0.182(1)/0.318(2) for Nd(1), 0.206(1)/0.294(2) for Nd(2), 0.209(1)/0.291(2) for Nd(3) and 0.259(2)/ 0.241(1) for Nd(4).

**Wavelength Dispersive Spectroscopy (WDS) Analyses.** Wavelength dispersive spectroscopy was used for quantitative chemical analysis to confirm the composition of **2**. An ETEC Autoprobe with Tracor Northern TN-2000 automation was used for spectrometer movement and data reduction. The acceleration voltage was set at 15 keV; the specimen current, measured in a stage mounted faraday cup, was adjusted to 20 nA; and the counting times were 30 s for both the standards and the samples. Data acquisition was accomplished using three scanning spectrometers. The intensities of each of the X-ray emissions of the samples were compared with those of a standard. The standards used for the analyses were Wollastonite,[14a] rare-earth glass standard no. 2,[14b] InAs (Tousimis), and Se metal (Tousimis). The compositions were calculated on-line using the ZAF program provided by Tracor Northern. The normalized composition of these analyses is consistent with the X-ray diffraction (XRD) study, *i.e.*, Ca:Nd:In:Se = 3.7:2.2:4.2:13 (WDS) vs 3.7:2.3:4.0:13 (XRD).

**Powder X-ray Diffraction.** The polycrystalline materials prepared in an exact stoichiometry, $Ca_4(RE)_2In_4Q_{13}$, were examined at room temperature by a Philips PW 1840 diffractometer equipped with Cu

(11) Sheldrick, G. M. In *Crystallographic Computing 3*; Sheldrick, G. M., Krüger, C., Goddard, R., Eds.; Oxford University Press: London/New York, 1985; pp 175−189.
(12) TEXSAN: Single Crystal Structure Analysis Software, version 5.0. Molecular Structure Corp., The Woodlands, TX, 1989.
(13) Zachariasen, W. H. *Acta Crystallogr.* **1968**, *A24*, 212.
(14) (a) Analytical Laboratory Report No. 72-WO-3. United States Geological Survey, **1972**. (b) Drake, M. J.; Weill, D. F. *Chem. Geol.* **1972**, *10*, 179.

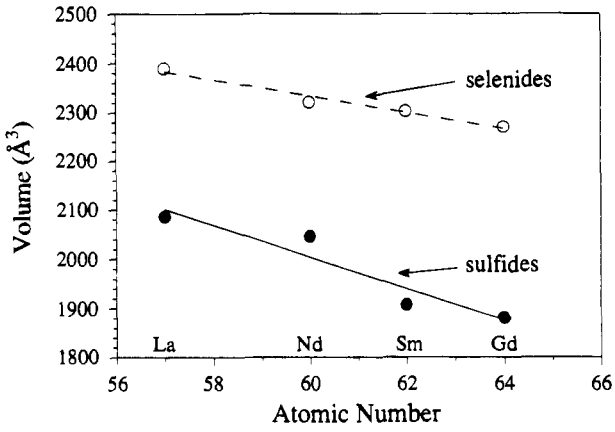


**Figure 1.** Volume vs atomic number plot for the $Ca_4(RE)_2In_4Q_{13}$ series. The straight lines indicate the linear fit of the relationship.

**Table 3.** Lattice Parameters for $Ca_4(RE)_2In_4Q_{13}$ (RE = La, Nd, Sm, Gd; Q = S, Se)

| compound | $a$, (Å) | $b$, (Å) | $c$, (Å) | $V$, Å$^3$ |
|---|---|---|---|---|
| | | Sulfides | | |
| $Ca_4La_2In_4S_{13}$ | 20.561(3) | 25.716(6) | 3.9447(4) | 2086(5) |
| $Ca_4Nd_2In_4S_{13}$ | 20.440(5) | 25.456(6) | 3.933(1) | 2046.1(9) |
| $Ca_4Sm_2In_4S_{13}$ | 20.291(8) | 25.054(8) | 3.754(2) | 1908(1) |
| $Ca_4Gd_2In_4S_{13}$ | 20.213(5) | 24.818(7) | 3.749(2) | 1881(1) |
| | | Selenides | | |
| $Ca_4La_2In_4Se_{13}$ | 21.532(7) | 26.796(8) | 4.142(1) | 2390(1) |
| $Ca_4Nd_2In_4Se_{13}$ | 21.349(4) | 26.544(7) | 4.0964(5) | 2321.4(8) |
| $Ca_4Sm_2In_4Se_{13}$ | 21.356(5) | 26.49(1) | 4.072(3) | 2304(2) |
| $Ca_4Gd_2In_4Se_{13}$ | 21.248(3) | 26.349(4) | 4.0567(9) | 2271.1(7) |

Kα radiation and a Ni filter. NIST (National Institute of Standards and Technology) silicon internal standard was mixed with the sample. The diffraction patterns, which showed no extra reflections, were indexed and the cell constants were refined by the least-squares program LATT[15] with ca. 30 reflections used. The lattice parameters for the $Ca_4(RE)_2In_4Q_{13}$ family are summarized in Table 3. The cell parameters from single-crystal indexing of **1**−**4** and the refined PXRD of the corresponding polycrystalline materials are in excellent agreement. This suggests that the $x = 2.0$ value in the $Ca_{2+x}(RE)_{4-x}In_4Q_{13}$ formula is appropriately assigned. In Figure 1, a linear relationship between the cell volume and the RE cation atomic number is shown. This demonstrates the correlation between the adaptive nature of the framework and the trend in size of the corresponding lanthanide series.

**Thermal Analysis.** Phase transformations of the prepared phases were studied by differential thermal analysis (DTA) in sealed quartz ampoules under vacuum. The thermal stabilities, in terms of the thermal decomposition in an oxygen atmosphere, were investigated by thermogravimetric analysis (TGA) under flowing oxygen. The decomposition temperature ($T_d$) was defined as the onset point of deviation on the weight vs temperature curve. Selected crystals were ground for both DTA and TGA experiments. The analyses were performed with a Du Pont 9900 thermal analyzer system using a heating rate of 10 °C per minute. The DTA and TGA results are summarized in Table 4.

All the DTA results suggest a congruent melting behavior as they show a reversible phase transformation with respect to melting. The melting point ($T_m$) of the sulfide is higher than the corresponding selenide as expected due to the bond interaction of sulfides being stronger than selenides.

In contrast to the trend observed in $T_m$, anomalies in the thermal decomposition behavior were observed. The measured $T_d$ is lower for the sulfide than the corresponding selenide, and the respective TGA curves show a weight gain vs a weight loss, as shown in Figure 2 for the example of $Ca_4Nd_2In_4Q_{13}$. From the analysis, the $T_d$ values are 457 and 681 °C for Q = S and Se, respectively. For the selenide phase, on the basis of total weight change the ultimate decomposition products are complex oxides. However, a positive deviation occurring in the TGA curve of the $Ca_4Nd_2In_4S_{13}$ phase is observed, which is attributed to the oxidative decomposition of sulfide to sulfate. The insert shows the characteristic infrared spectra of sulfate, which was observed in all of the TGA products of the $Ca_4(RE)_2In_4S_{13}$ sulfide series. An early onset temperature, accompanied by the oxidative decomposition, is observed in the sulfide phases.

(15) Takusagawa, F. Ames Laboratory, Iowa State University, Ames, IA, Unpublished research, 1981.

**Table 4.** Summary of Melting Point ($T_m$, °C), Decomposition Temperature ($T_d$, °C), and Bandgap ($E_g$, eV) of the $Ca_4(RE)_2In_4Q_{13}$ Series (RE = La, Nd, Sm, Gd; Q = S, Se)

| compound | $T_m$ | $T_d$ | $E_g$[a] |
|---|---|---|---|
| | Sulfides | | |
| $Ca_4La_2In_4S_{13}$ | 1219 | 454 | |
| $Ca_4Nd_2In_4S_{13}$ | 1191 | 457 | 2.0 |
| $Ca_4Sm_2In_4S_{13}$ | 1158 | 421 | 1.8 |
| $Ca_4Gd_2In_4S_{13}$ | 1161 | 419 | 2.0 |
| | Selenides | | |
| $Ca_4La_2In_4Se_{13}$ | 1062 | 583 | |
| $Ca_4Nd_2In_4Se_{13}$ | 1016 | 681 | |
| $Ca_4Sm_2In_4Se_{13}$ | 969 | 573 | 1.3 |
| $Ca_4Gd_2In_4Se_{13}$ | 974 | 799 | 1.2 |

[a] Bandgaps of some reference materials were measured showing a close match between the observed and reported values, *e.g.*, 3.0/3.1 eV ($TiO_2$), 2.6/2.6 eV (ZnSe), and 1.1/1.1 eV (Si). Five of the title compounds were measured for optical bandgaps.

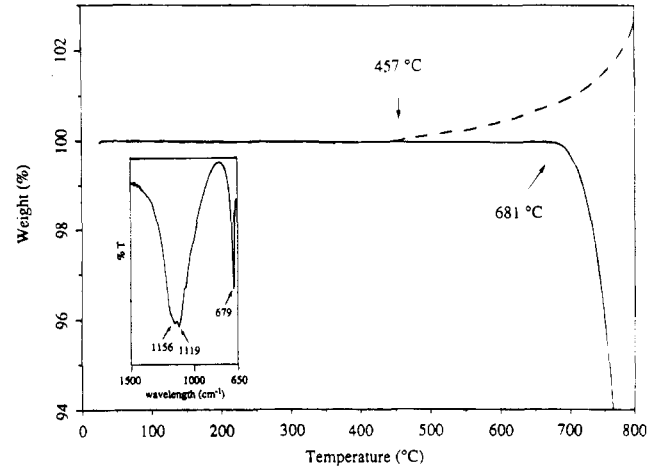


**Figure 2.** TGA curves of $Ca_4Nd_2In_4Q_{13}$, where Q = S (dotted line) and Se (solid line), with onset temperatures marked. The inset is an infrared spectra of sulfate observed in the TGA product; see text.

**Infrared and UV/vis Spectroscopy.** The infrared spectra of the title compounds were obtained from diffuse reflectance infrared fourier transform spectroscopy (DRIFTS), using the procedures described previously.[2c] The obtained spectra (4000−400 cm$^{-1}$) of ground single crystals showed only weak absorption bands due to water. Polycrystalline samples also examined showed no absorption bands in the analyzed range, suggesting the above bands correspond to residual water from washing. Otherwise, the title compounds are transparent in the IR region.

Preliminary optical bandgap evaluations of some selected quaternary chalcogenides were also performed in the UV/vis region by reflectance spectroscopy. The obtained spectra were interpreted using methods described before.[2c] As listed in Table 4, the results of the investigation suggest these materials are medium-gap semiconductors with $E_g$ of ~2.0 eV for sulfides and ~1.2 eV for selenides.

## Structure Description and Discussion

The three-dimensional framework consists of Ca−Q octahedra, (Nd,Ca)−Q bicapped trigonal prisms, and In−Q tetrahedra and octahedra. Figure 3 shows the perspective view of the unit cell of the representative lattice, $Ca_4Nd_2In_4Se_{13}$, as an ORTEP[16]

(16) Johnson, C. K. *ORTEP II*; Report ORNL-5138; Oak Ridge National Laboratory: Oak Ridge, TN, 1976.

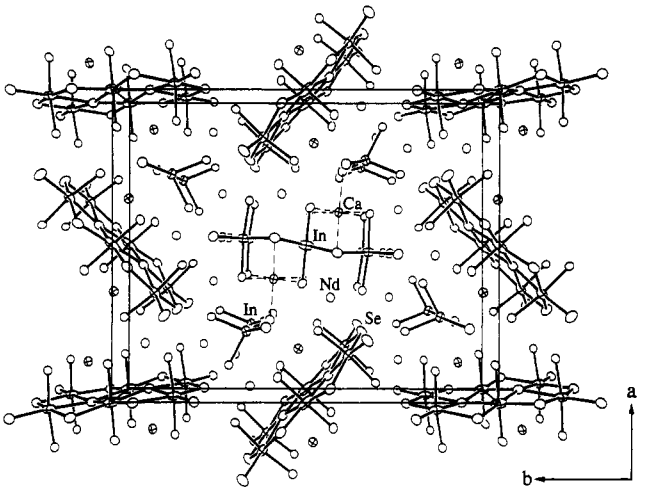


**Figure 3.** Perspective view of the $Ca_4Nd_2In_4Se_{13}$ unit cell viewing down along the *c* axis. The In−Se tetrahedra and octahedra are outlined by In−Se bonds (solid lines). For clarity, only two of the Ca−Se octahedra are drawn in dotted lines to show the relative orientation. The Nd positions are represented by nonbonded open circles. The anisotropic thermal ellipses here, and in all figures, are presented in 90% probability.

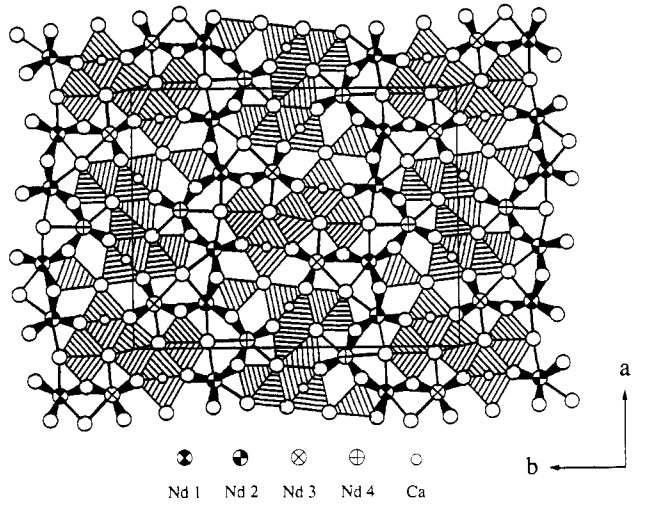


**Figure 4.** STRUPLO polyhedral plot of a projected view of the $Ca_4Nd_2In_4Se_{13}$ unit cell. The Nd sites are shown in large hatched circles while the Ca and Se are in small and large open circles, respectively. The In cations centered in $InSe_4$ and $InSe_6$ are omitted for simplicity.

drawing. The structure is composed of infinite octahedral ribbon three $InSe_6$ units wide, adopting the NaCl type extending along *c*. The two Ca cations are positioned opposite to each other about the center of the octahedral sheet. As shown in the polyhedral drawing in Figure 4, the $CaSe_6$ octahedra are fused to the sheet through shared cis edges. The $CaSe_6$ octahedra share apical Se to interconnect the neighboring sheets along *a*, and trans edges along the viewing direction *c* with neighboring $CaSe_6$ octahedra to form an infinite chain. The fused Ca−Se and In−Se polyhedra, with the In−Se tetrahedra, form extended polyhedral bands centered around the (020) planes. The four independent Nd cations are in the rows of interstitial sites adopting bicapped trigonal prismatic geometry.

As shown in Figure 5, two independent octahedral units are interconnected through Se(12), a shared-corner with two In(4)-$Se_4$ tetrahedra. The formula of each independent unit is $Ca_2In_6Se_{26}$, consisting of eight edge-shared octahedra, *i.e.*, (two Ca(1)$Se_6$, four In(1)$Se_6$, two In(2)$Se_6$) and (two Ca(2)$Se_6$, four In(3)$Se_6$, two In(5)$Se_6$). The inversion center is located at the point halfway between the two middle indiums along the

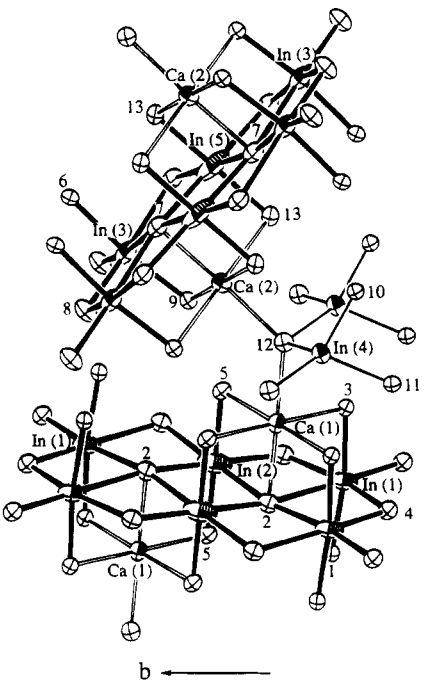


**Figure 5.** ORTEP drawing of two independent $Ca_2In_6Se_{26}$ octahedral units corner-shared with two In(4)$Se_4$ tetrahedra at Se(12). The thin and thick solid lines represent In−Se bonds in $InSe_4$ and $InSe_6$, respectively. The hollow lines represent Ca−Se bonds in $CaSe_6$. The cations are represented by shaded thermal ellipses. The Se atoms are labeled numerically for clarity.

viewing direction, *e.g.*, two In(2) and two In(5), respectively. It is noted that Se(12) is coordinated to four cations, while the remaining 12 independent seleniums adopt higher coordination numbers, 5−8.

The title compounds are isostructural with the $Pb_4In_2Bi_4S_{13}$ phase,[17] whose unit cell is not well described. On the basis of atomic coordinates comparison, its structural formula can be written as $(Bi_2Pb_x)Pb_{4-x}(In_2Bi_2)S_{13}$ ($x = 2$). The corresponding octahedral unit consists of two $BiS_6$ capping octahedra and a mixed $BiS_6$−$InS_6$−$BiS_6$ octahedral sheet. It is found that the octahedral unit is a feature commonly shared by other known compounds, *e.g.*, $Pb_3In_{6.67}S_{13}$,[18] and $Ca_{3.1}In_{6.6}S_{13}$.[19] These two phases possess an additional structural unit of seven edge-shared octahedra forming stepped layers.

Table 5 lists the important bond distances for the $Ca_4Nd_2In_4Se_{13}$ structure. The bond distance ranges for Ca(1)$Se_6$/Ca(2)$Se_6$ and In(4)$Se_4$ are narrow, *e.g.*, 2.88−2.95 Å and 2.56−2.58 Å, respectively. In contrast, the bond distances for the four independent $InSe_6$ octahedra are relatively diverse, *e.g.*, 2.58−3.05 Å, which indicates that these $InSe_6$ octahedra are distorted. For the two outside octahedra, In(1)$Se_6$ and In(3)-$Se_6$, of the above-mentioned octahedral unit, the indium to apex selenium distances are distinctively longer than the waist distances. This trend is reversed for the inside octahedra, In(2)$Se_6$ and In(5)$Se_6$. Such a distortion is commonly seen in many ternary indium sulfide compounds, *e.g.*, $Pb_3In_{6.67}S_{13}$,[18] $Ca_{3.1}In_{6.6}S_{13}$,[19] $Sm_3InS_6$,[20a] $Tb_3In_5S_{12}$,[20b] and $Nd_4In_5S_{13}$,[20c] and binary indium selenide compounds, *e.g.*, $In_6Se_7$.[21] The observed bond distances are, however, consistent with the sum of the

(17) Krämer, V. *Acta Crystallogr.* **1986**, *C42*, 1089.
(18) Ginderow, D. *Acta Crystallogr.* **1978**, *B34*, 1804.
(19) Chapuis, G.; Niggli, A. *J. Solid State Chem.* **1972**, *5*, 126.
(20) (a) Messain, D.; Carré, D.; Laruelle, P. *Acta Crystallogr.* **1977**, *B33*, 2540. (b) Carré, D. *Acta Crystallogr.* **1977**, *B33*, 1163. (c) Gusejnov, G. G.; Mamedov, F. Kh.; Shnulin, A. N.; Mamedov, Kh. N. *Dokl Akad Nauk SSSR* **1979**, *246*, 1360.
(21) Hogg, J. H. *Acta Crystallogr.* **1971**, *B27*, 1630.

**Table 5.** Important Bond Distances (Å) for $Ca_4Nd_2In_4Se_{13}$

| | | | |
|---|---|---|---|
| Nd(1)−Se (1)[a,b] | 3.010(2) (2×) | Ca (1)−Se (5)[a,b] | 2.922(3) (2×) |
| Nd(1)−Se (4)[a] | 3.129(2) | Ca (1)−Se (12)[a] | 2.912(4) |
| Nd(1)−Se (8)[a] | 3.107(2) | Ca (2)−Se (7)[k] | 2.879(4) |
| Nd(1)−Se (10)[a,b] | 3.109(2) (2×) | Ca (2)−Se (9)[j,k] | 2.909(3) (2×) |
| Nd(1)−Se (11)[a,b] | 3.070(2) (2×) | Ca (2)−Se (12)[a] | 2.901(4) |
| Nd(2)−Se (3)[a,b] | 3.064(2) (2×) | Ca (2)−Se (13)[a,b] | 2.947(3) (2×) |
| Nd(2)−Se (4)[c] | 3.189(2) | In (1)−Se (1)[a] | 2.645(2) |
| Nd(2)−Se (6)[a,b] | 3.015(2) (2×) | In (1)−Se (2)[a,h] | 3.052(2) (2×) |
| Nd(2)−Se (8)[a] | 3.275(3) | In (1)−Se (3)[f] | 2.628(2) |
| Nd(2)−Se (11)[a,b] | 3.072(2) (2×) | In (1)−Se (4)[a,h] | 2.686(2) (2×) |
| Nd(3)−Se (1)[a,b] | 3.017(2) (2×) | In (2)−Se (2)[i,c,j,k] | 2.929(2) (4×) |
| Nd(3)−Se (2)[a] | 3.237(2) | In (2)−Se (5)[a,l] | 2.606(2) (2×) |
| Nd(3)−Se (5)[d,e] | 3.075(2) (2×) | In (3)−Se (6)[a] | 2.668(2) |
| Nd(3)−Se (9)[a,b] | 3.062(2) (2×) | In (3)−Se (8)[a,h] | 2.660(2) (2×) |
| Nd(3)−Se (8)[a] | 3.335(3) | In (3)−Se (7)[a,h] | 3.068(2) (2×) |
| Nd(4)−Se (4)[a] | 3.276(3) | In (3)−Se (9)[a] | 2.652(2) |
| Nd(4)−Se (6)[f,g] | 3.004(2) (2×) | In (4)−Se (10)[a] | 2.575(2) |
| Nd(4)−Se (7)[g] | 3.151(3) | In (4)−Se (12)[a,h] | 2.577(2) (2×) |
| Nd(4)−Se (10)[a,b] | 3.060(2) (2×) | In (4)−Se (11)[a] | 2.579(2) |
| Nd(4)−Se (13)[a,b] | 3.091(2) (2×) | In (5)−Se (7)[a,h,m,n] | 2.962(2) (4×) |
| Ca (1)−Se (2)[c] | 2.895(4) | In (5)−Se (13)[d,i] | 2.580(2) (2×) |
| Ca (1)−Se (3)[a,b] | 2.906(3) (2×) | | |

[a] Symmetry codes: (a) $x, y, z$; (b) $x, y, 1 + z$; (c) $-1/2 + x, 1/2 - y, 1 - z$; (d) $1/2 - x, 1/2 + y, -z$; (e) $1/2 - x, 1/2 + y, 1 - z$; (f) $1/2 + x, 1/2 - y, -z$; (g) $1/2 + x, 1/2 - y, 1 - z$; (h) $x, y, -1 + z$; (i) $-1/2 + x, 1/2 - y, -z$; (j) $1/2 - x, -1/2 + y, -z$; (k) $1/2 - x, -1/2 + y, 1 - z$; (l) $-x, -y, z$; (m) $-x, 1 - y, -1 + z$; (n) $-x, 1 - y, z$.

Shannon crystal radii[22] as well as those reported in the literature, such as 2.91−2.99 Å for Ca−Se and 2.53−2.61 Å for 4 CN In−Se in $CaYbInSe_4$,[2c] and 2.61 Å ~ 3.00 Å for 6 CN In−Se in $In_6Se_7$.

In contrast to the coordination of Pb in the $Pb_4In_2Bi_4S_{13}$ structure, which reside in both mono- and bicapped trigonal prismatic sites, the corresponding Nd in the title compounds are found uniformly in a bicapped trigonal prism (bTP). Figure 6 presents two face-shared Nd(3)$Se_8$ bTPs, stacking along the $c$ axis. It is shown that there is a distinct difference in the capping vs vertex Nd−Se bond distances, *i.e.*, 3.237−3.335 Å vs 3.017−3.075 Å, respectively. The longer capping selenium distances assume a weaker electrostatic interaction with the trivalent neodymium center. Thus the two capping Se atoms are regarded as "outer-sphere" coordinates with respect to the trigonal prism. It is noted in Table 5 that the Nd(1)−Se bond distances are quite similar, but the capping Se(4) and Se(8) atoms still have distances at the longer end of the range. The inner-sphere Nd−Se distances are comparable with the sum (3.089 Å) of the Shannon crystal radii of eight-coordinated neodymium, $Nd^{3+}$ (1.249 Å), and six-coordinated selenium, $Se^{2-}$ (1.84 Å).

It is significant to realize that the presently studied quaternary chalcogenide phases, $Ca_4(RE)_2In_4Q_{13}$, are found in the proximity of the phase compatibility region for attempts to prepare analogs of the olivine family, $CaYbInQ_4$. The frameworks of these two series of quaternary compounds are drastically different; *i.e.*, the present structure is less compact than the olivine series which has a close-packed structure. Like in the above discussed ternary rare-earth chalcogenides, the size of the RE cation seems to play a determining role on the type of structure adopted by the material. More specifically, the early lathanides seem to adopt trigonal prismatic geometry while the late lanthanides adopt octahedral geometry in the Ca−RE−In−Q systems. This may lead to the failure of the olivine structure to form in the current systems, even though the atomic ratios of anions to the sum of cations are similar, *e.g.*, 1.30 and 1.33, respectively. Detailed analysis concerning the structure turnover point is planned.

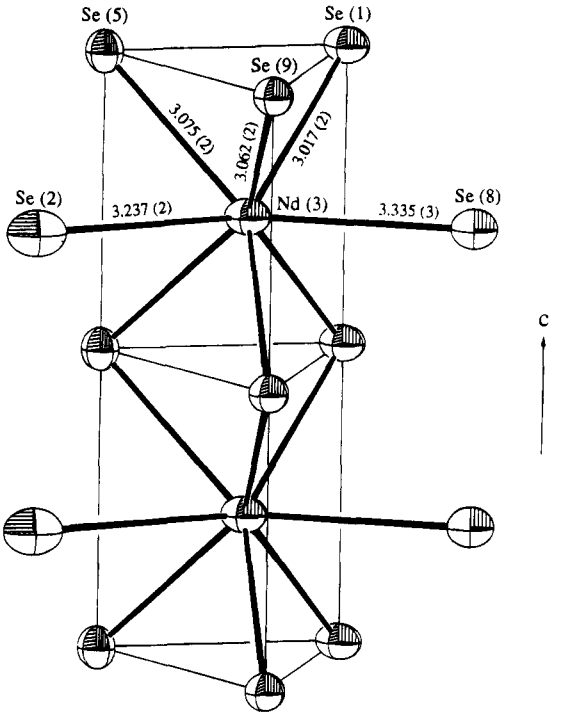


**Figure 6.** ORTEP drawing of two face-sharing Nd(3)$Se_8$ bicapped trigonal prisms.

Different structural packing may be responsible for the variation in observed $T_m$, $T_d$, and thermal behavior among these two families of quaternary chalcogenides. The previously reported $CaYbInQ_4$ phases are high melting ($T_m$ > 1200 °C) and decompose to oxides for both Q = S and Se at $T_d$ = 575 and 715 °C, respectively. The thermal decomposition of the $Ca_4(RE)_2In_4S_{13}$ sulfides proc eeds via oxidative decomposition, and, with an exception of $T_d$ = 799 °C for $Ca_4Gd_2In_4Se_{13}$, both $T_m$ and $T_d$ for the title compounds are notably lower. In any event, this new family of RE-containing chalcogenides are IR-transparent and have provided us the opportunity to perform structure/property correlation studies generating further understanding of the parameters that are important to the synthesis of better ceramics.

**Acknowledgment.** We are grateful for the financial support of this research by the Robert A. Welch Foundation. The authors are indebted to Mr. M. L. Pierson and Dr. J. C. Stormer, Jr., for microprobe analysis. Financial support for the single crystal X-ray diffractometer by the National Science Foundation is gratefully acknowledged.

**Supporting Information Available:** Tables of detailed crystallographic data for $Ca_4Nd_2In_4S_{13}$ and $Ca_4(RE)_2In_4Se_{13}$ (RE =Nd, Sm, Gd), atomic coordinates and anisotropic thermal parameters, bond distances and angles, indexed powder patterns for $Ca_4Nd_2In_4Se_{13}$ (31 pages). Ordering information is given on any current masthead page.

IC950265S

(22) Shannon, R. D. *Acta Crystallogr.* **1976**, *A32*, 751.